Modulating sustained drug release from nanocellulose hydrogel with the geometry of implantable capsules

Vili-Veli Auvinen[1,2*], Juhani Virtanen[3], Arto Merivaara[2], Valtteri Virtanen[3], Sampo Tuukkanen[3], Timo Laaksonen[1]

[1]Faculty of Engineering and Natural Sciences, Tampere University, P.O. Box 541, 33014 Tampere, Finland

[2]Division of Pharmaceutical Biosciences, Faculty of Pharmacy, University of Helsinki, P.O. Box 56, FI-00014, Finland

[3]Faculty of Medicine and Health Technology, Tampere University, P.O. Box 692, 33101 Tampere, Finland

[*]Corresponding author

Email: vili.auvinen@tuni.fi

Tel. +358 294159131

Tampere University, P.O. Box 541, 33014 Tampere, Finland

Abstract

Nanocellulose hydrogel has been shown to be an excellent platform for drug delivery and it has been lately studied as an injectable drug carrier. 3D printing is an effective method for fast prototyping of pharmaceutical devices with unique shape and cavities enabling new types of controlled release. In this study, we combined the versatility of 3D printing capsules with controlled geometry and the drug release properties of nanocellulose hydrogel to accurately modulate its drug release properties. We first manufactured non-active capsules via 3D printing from biocompatible poly(lactic acid) (PLA) that limit the direction of drug diffusion. As a novel method, the capsules were filled with a drug dispersion composed of model compounds and anionic cellulose nanofiber (CNF) hydrogel. The main benefit of this device is that the release of any CNF-compatible drug can be modulated simply by modulating the inner geometry of the PLA capsule. In the study we optimized the size and shape of the capsules inner cavity and performed drug release tests with common beta blockers metoprolol and nadolol as the model compounds. The final results demonstrate that the sustained release profiles provided by the CNF matrix can be accurately modulated via adjusting the geometry of the 3D printed PLA capsule, resulting in adjustable sustained release for the model compounds.

Keywords: 3D printing, nanocellulose, hydrogel, sustained drug release

1 Introduction

The increased access to 3D printers has accelerated the development of new products and applications for drug release device development on the pharmaceutical field. These breakthroughs include 3D printing bilayers of different medicinal compounds into an oral single dosage form, oral tablets with inner channels and porous structures and adjustments on the geometry of printed oral capsules allowing customization of the drug release [1-5]. However, the usage of such geometrical innovations has not yet boomed on the rapidly growing market of implantable polymeric drug release devices [6]. These devices can be classified into four groups: passive polymeric implants, non-biodegradable polymeric implantable systems, biodegradable implants and dynamic or active implants [6]. In addition, the drug release mechanisms from such devices can be classified into four categories: controlled swelling, matrix degeneration, passive diffusion and osmotic pumping [7]. Controlled swelling, passive diffusion and matrix degeneration have a key role in monolithic and reservoir type implants, which have been illustrated in Figure 1 [6]. In osmotic type implants, a non-permeating polymer is used and the osmotic gradient creates a stable inflow of body fluid within the device [8]. This increases the pressure inside the implant and forces drug release trough the opening as shown in figure 1 [8]. Such design produces a constant drug release with zero order kinetics [8]. Some monolithic implants feature no solid structures, but instead rely on injectable drug releasing hydrogel formulations. Two recent interesting applications are a nanogel-based *in situ* forming implant for HIV drug release [9] and an application where CNF hydrogel formulations were subcutaneously injected in mice [10]. The injected CNF hydrogels operated as a monolithic type implant, as the hydrogel had a high loading and it did not migrate or dilute despite the free movement of the mice [10]. In our work, we studied the use of a CNF hydrogel formulation as monolithic drug dispersions but inside a combination

type implant illustrated in Figure 1. Successful clinical testing has recently been performed with a similar device, comprising of a simple cylindrical capsule filled with a 2-hydroxyethyl methacrylate hydrogel and a therapeutic agent [11].

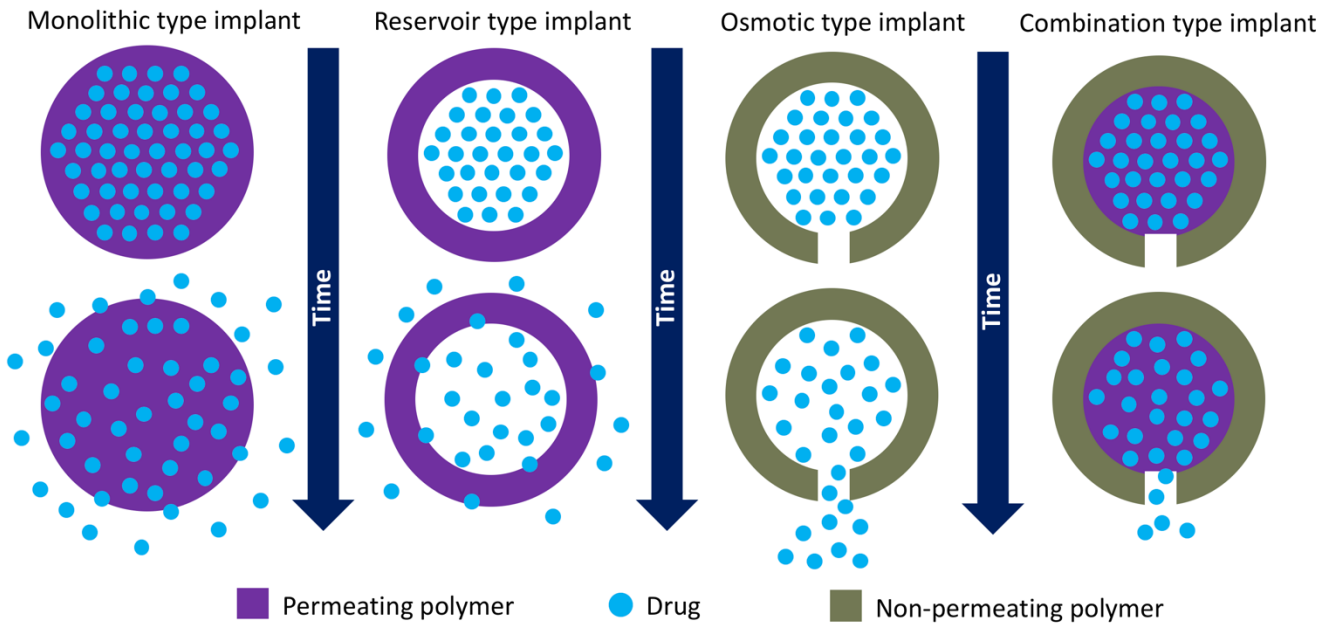

Fig 1. An illustration of monolithic, reservoir, osmotic and combination type implants.

Cellulose-based nanostructured materials, generally known as a family of nanocelluloses, are interesting biocompatible materials, which have shown benefits in numerous medical applications [12]. Nanocellulose can be produced in three types: as bacterial cellulose (BC), nanocrystals (CNC) and as cellulose nanofibers (CNF) [13]. The cellulose nanofibers can be chemically modified by TEMPO [(2,2,6,6-tetramethylpiperidin-1-yl)oxyl] oxidation to manufacture anionic cellulose nanofibers [14, 15]. Lately, anionic CNF hydrogels have been shown to operate as a semi-universal drug matrix for the release of different types of molecules (small, large, cationic

and anionic) [16, 17]. In addition, CNF has been used to manufacture drug-loaded film-like matrix systems with long-lasting sustained release for up to three months [18].

3D printing typically involves heat or other manufacturing methods that limit its suitability for biomolecules, such as proteins and lipids during the manufacturing process [19]. The 3D printed drug delivery systems might further have an uneven or porous surface affecting the rate of the drug release, especially in extrusion and powder printing [20]. Extrusion, powder and inkjet-based printing require post-operative drying, which is an additional process variable affecting the appearance and the properties of the product [21]. However, it is possible to overcome these limitations by first printing customized capsules from an inert biocompatible material, and then fill the capsules with the sensitive drugs or biomolecules together with a rate-controlling matrix material [22]. It is also possible to subsequently print a drug dosing cap to furtherly enhance and modulate the sustained release profile [19, 22]. For implementation of drug release devices there are typically three main sites: subcutaneous, intra-vaginal and intra-vesical. [6] The usage of subcutaneous drug releasing devices is an invasive process and typically leaves scarring to the patient. However, in some cases this is still a preferred treatment option compared to continuous injections or daily pills or the drug implant has other benefits compared to oral dosing such as in the complex case of opioid addicted patients [23, 24].

In this study, we combine the new possibilities of printing specifically designed drug capsules and the recent advances in the implantation of CNF hydrogels into three rapid prototyped designs and evaluate their properties *in vitro* as sustained release devices. Traditionally in pharmaceutical hydrogel applications, the release rate of the drug is controlled by the concentration of the loaded

drug and other active ingredients [25]. Here, a similar effect is expected by controlling the geometry of the outer capsule which limits drug diffusion from the hydrogel. The idea differs from the previously mentioned drug release devices and hydrogels as the release is fundamentally controlled by the inner hydrogel, which facilitates a sustained release profile while the release can be further modulated via the geometry of the inner cavity of the capsule.

2 Materials and Methods

2.1 Materials

2.7% (lot 11724) anionic CNF hydrogel Fibdex^{TM} was purchased from UPM-Kymmene Oyj, Finland. Primavalue PLA filaments were purchased from 3D Prima, Mälmö, Sweden. Nadolol, metoprolol tartrate and methylene blue, were purchased from Sigma-Aldrich, USA. Dulbecco's Phosphate Buffered Saline (10×) concentrate without calcium and magnesium was purchased from Gibco, UK. The buffer solution used was made in double distilled ultrapure water.

2.2 Printing of PLA capsules

The capsules were modeled with Onshape (Onshape inc, Cambridge, USA) Computer Aided Design (CAD) software and the CAD model was later processed with Slic3r -software package to produce the actual printing data. Capsules were printed from commercially available PLA filaments using fused deposition modeling (FDM) printing process. The FDM process is essentially an extrusion method where a heated material, in this case PLA, is directed through a nozzle and deposited in x, y and z space to form structures. In this particular printing case, the capsules were printed with 100% infill to ensure the sufficient barrier properties of the printed walls. The used printing layer height was 0.2 mm and the 3D printing was carried out using PRUSA I3 MK2 (Prusa research, s.r.a., Praha, Czech republic) 3D printer at 210 °C and at the printing rate of 40 mm/s. The printer nozzle diameter during the printing was 0.4 mm. No post processing, such as smoothing after the printing, was performed, however each capsule used in the experiments was hand-picked so that no visible unevenness around the release channel could be observed. The printing method was FDM type of extrusion of material through a hot nozzle. The length of each produced capsule was 20 mm, and the width 10 mm. The diameter of the bottleneck

was 2.0 mm for small, 3.6 mm for large and 5.0 mm for tube design leading into shared constant flat surface areas of 3.1 mm^2 for small, 10 mm^2 for large and 19 mm^2 for the tube design. The inner total volumes were 360 mm^3 for the small, 430 mm^3 for the large and 330 mm^3 for the tube design.

2.3 Leakage tests and injection of hydrogel formulations

After the manufacturing of the capsules, leakage tests were performed using methylene blue as a dye for visual observation of possible leaks. First, a dyed hydrogel was made by mixing anionic CNF hydrogel with methylene blue and injecting it inside the capsules with standard 19G needles. The capsules were weighted before and after injection to ensure that a complete filling had been accomplished and to rule out the presence of air bubbles. Next, the capsules were wet and any leakage of the blue color trough the core was observed with a slow-motion camera.

2.4. Preparation of the hydrogel formulations

The hydrogel formulations were prepared by mixing anionic CNF hydrogel with the model compounds. The mixing was performed by connecting two 10 ml syringes from their nozzles with a tiny rubber hose and then pushing the contents of each syringe to the other via the hose. The anionic CNF hydrogel (fiber content 2.7%) was weighted directly in the syringes and nadolol or metoprolol was added as a dry powder. Nadolol and metoprolol were loaded in excess amount to form monolithic dispersions. The formulations were then homogenized by pushing the contents back and forth trough the hose for 5 min. The final amount of cellulose nanofibers in both formulations was ~1.8 %. The total amount of metoprolol inside the capsules was 152 mg for the large design, 130 mg for the small design and 105 mg for the tube design. For nadolol, the amounts were 131 mg for the large capsule, 110 mg for the small design and 91 mg for the tube design. The

used quantity for nadolol represents concentration of 0.89 M. The solubility of nadolol in water is 0.03 M, meaning that the water-based hydrogel formulation can be characterized as a monolithic dispersion [26]. The solubility for metoprolol tartrate in water is much higher and hence it's solubility in the 2.7% ANFC hydrogel was tested separately with nephelometry. The results show that the hydrogel does not possess enough free water to dilute all of the added metoprolol, resulting in a monolithic dispersion. The measured solubility data for metoprolol is shown in the supplementary data.

2.5 In vitro drug release studies

The 3D printed capsules were filled with formulated hydrogels via injection with standard 19G needles and the visible hydrogel surface was evened with plastic strips. The capsules were weighted before and after injection to ensure that a complete filling had been accomplished and to rule out the presence of air bubbles. The filled capsules were placed in glass bottles with 70 ml of phosphate buffered saline (1 x DPBS) and kept at 37 °C incubator shaker (Innova 4400, by ALLERGAN. Inc.) under constant shaking at 150 RPM for 3 weeks, except the small and large designs for nadolol were measured for 5 weeks. At chosen time points, 1 ml of sample was collected from each sample and replaced with 1 ml of fresh buffer. The amount of removed model compound from each time point was mathematically added to the next time point in order to plot cumulative release. All experiments were performed in triplicate.

2.6 Quantification of released model compounds

The concentrations of nadolol and metoprolol from the in vitro release tests were analyzed with Ultra performance liquid chromatography (UPLC) instrument Acquity UPLC (Waters, USA). For

nadolol and metoprolol, the used column was HSS-T3 1.8 μm (2.1 × 50 mm) (Waters, USA) at 30 °C. The injection volume for nadolol was 5 μl and for 2 μl for metoprolol and the flow rate was 0.5 ml/min for both compounds. The detection of nadolol and metoprolol was performed at the wavelengths of 215 nm and 221 nm, respectively. During the gradient run the mobile phase consisted of a mixture of acetonitrile and 15 mM phosphate buffer at pH 2 in 10:90 ratio for nadolol and 20:80 for metoprolol. The retention times were 0.92 min for nadolol and 0.89 min for metoprolol.

3 Results and Discussion

We designed capsules that had an inner cavity, or a reservoir, for the CNF hydrogel, and a single release channel (to which we will be later referring as bottleneck). Outer measurements for each design were 10 mm x 20 mm and the capsules were 3D printed from poly(lactic acid) (PLA) using fused deposition modelling (FDM) and filled with a suspension made of anionic CNF hydrogel and the model compounds, nadolol and metoprolol, which are both commonly used beta blockers. Nadolol's release profile from anionic CNF hydrogels have been characterized previously, where 90% of the loaded nadolol diffused out of the hydrogel during one week [16]. PLA and anionic CNF hydrogel were chosen as materials for the capsules, as both are biocompatible materials (in humans) and biodegradable (in nature) [27-30].

The designs of the manufactured capsules are visualized in Figure 2 (A-C) and with exact measurements in the supplementary material. The bottlenecks lead into inner cavities, which were filled with the anionic CNF hydrogel containing the studied model compound. We will refer to the different structures as small (Fig 2A), large (Fig 2B), and tube (Fig 2C) designs. The designs

198 presented here allow for a wide range of customization. As the PLA capsule carries and regulates
199 the open surface area of the anionic CNF hydrogel, which operates as a matrix for the model
200 compounds, the drug release can be controlled by modifying the characteristics of either
201 component. However, as the release properties of anionic CNF hydrogels has been established
202 previously [16], we focus on the geometry of the PLA capsule in this study and demonstrate that
203 flexible control over the release rate can be achieved with minimal changes to the inner matrix.
204

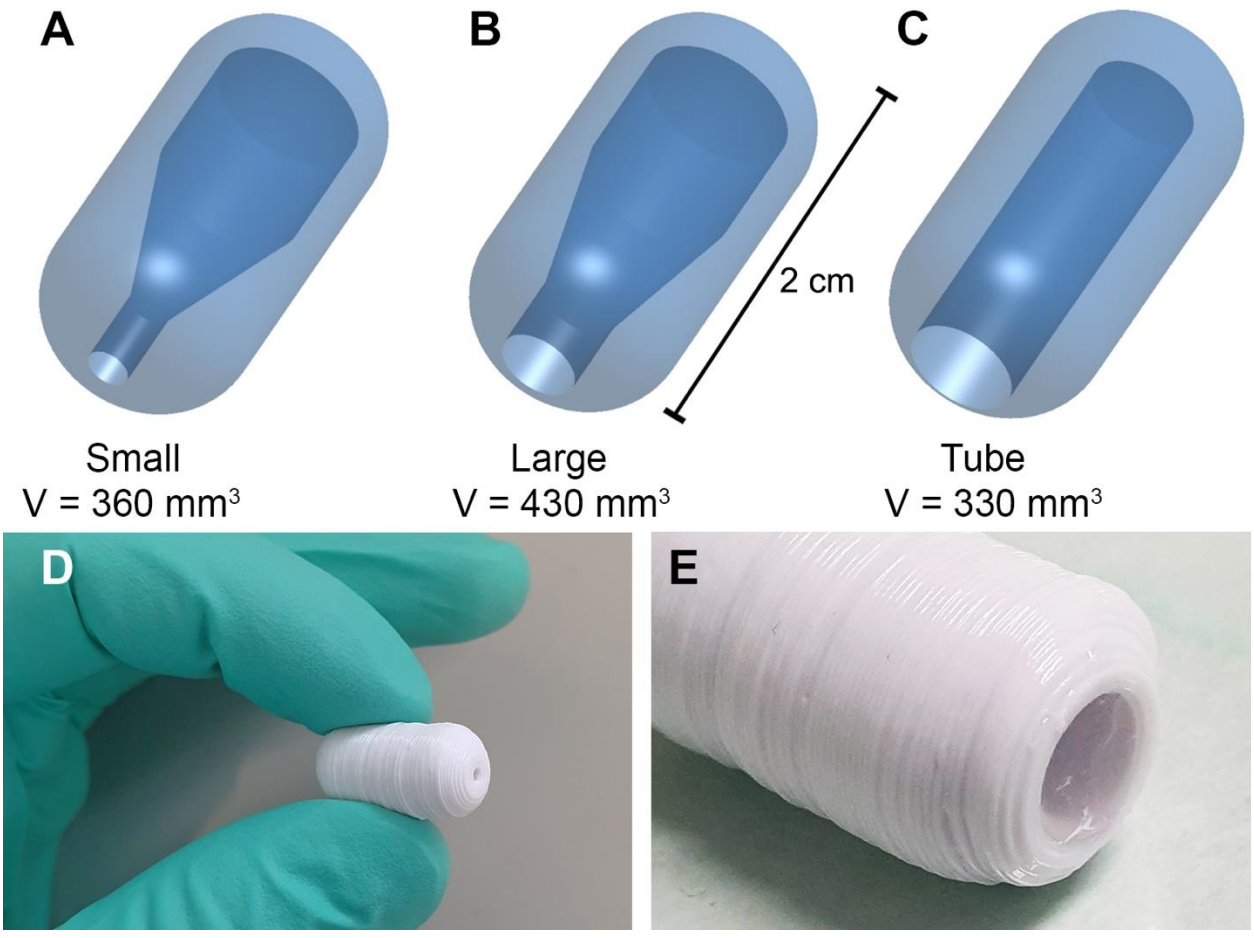

205

206 **Fig 2**. Computer aided designs (A-C) and physical printed versions (D-E) of the studied PLA
207 capsules. (A) Small capsule. (B) Large capsule. (C) Tube design. (D) A 3D printed PLA capsule

(small). (E) The tube design filled with a hydrogel (picture taken after 3 weeks in DPBS buffer) showing an even surface of the hydrogel.

3.1 Leakage tests and optimization of the PLA capsules

The designs were first optimized not to leak via prototyping. Figure 2 shows the final optimized designs. We particularly had to optimize the bottom thickness as our first designs with a thin bottom leaked from the edges of the inner cavities. The combination of 3D printing and separate injection of the hydrogel allowed bypassing any requirements set by the FDM printing such as the required flow properties of the drugs [31]. The model compounds metoprolol and nadolol did not undergo any temperatures above 37 °C during the study, suggesting that the method would be compatible with biomolecules such as lipids and proteins. The final optimized designs are presented in Figure 2 A-C and with exact measurements in the supplementary data.

3.2 Sustained in vitro release of the model compounds

During the three-week release study, a sustained release profile was obtained for both model compounds with all three PLA capsule designs. As expected, the small design with the smallest surface area in contact with the external buffer sustained the release the most for both model compounds. The large design had less effect on sustaining the release, and the tube design sustained the release the least, as expected. During the first hours all capsules released model compounds rapidly and the release rate became then more linear. For the tube design with metoprolol, the highest total release of 96.4% was reached on the 14^{th} day. The results are shown in Figure 3, where the top three lines represent the release of the metoprolol filled PLA capsules, and the bottom three the nadolol filled PLA capsules. No swelling nor collapsing of the hydrogels

were visually observed during the three-week measurements, as shown in Figure 2 E still showing an even surface of hydrogel, matching the results of Paukkonen et al. [16]. After 14 days, the amount of metoprolol in the buffer appeared to decrease (data not shown). This is due to the hydrolysis of nadolol and metoprolol in aqueous conditions [32]. However, in the case of nadolol, this was not observable due to extremely sustained release, which allows part of the drug to remain in crystallized form inside the hydrogel and hence delay the hydrolysis. As the hydrogels contained a significant amount of undissolved drug maintaining a constant activity source, the hydrogels can be characterized as monolithic dispersions. We performed solubility measurement for metoprolol in anionic CNF hydrogel with nephelometry and the results are shown in the supplementary data.

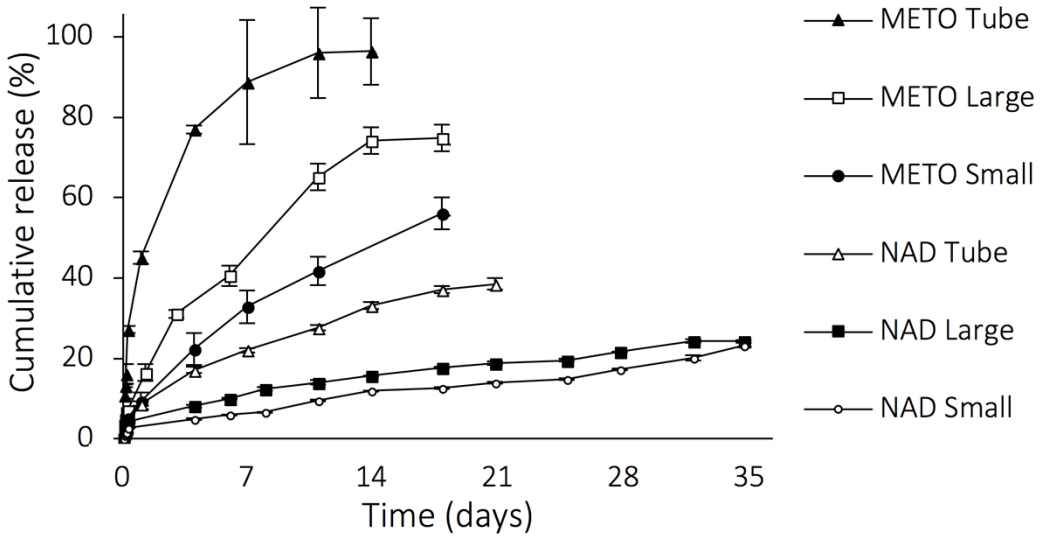

Fig 3. Scaled cumulative release of the model compounds metoprolol (METO) and nadolol (NAD) from the three capsule designs (Tube, Large, and Small) carrying anionic cellulose nanofiber hydrogel drug formulations (mean ± S.D., n = 3). The experiments were conducted at 37 °C in DPBS buffer.

3.2 Mathematical model for the release

For monolithic dispersions with flat release areas, the release rate is expected to follow the Higuchi equation (1) [33].

$$f = \frac{A}{M_{\text{loaded}}}\sqrt{Dc_{\text{s}}(2c_{\text{ini}} - c_{\text{s}}) \times t} = \frac{A}{V}\sqrt{Dc_{\text{s}}/c_{ini}^2(2c_{\text{ini}} - c_{\text{s}}) \times t} \quad (1)$$

where f is the fraction of the drug released, M_{loaded} is amount of the drug initially loaded into the capsule, A is the surface area exposed to the release buffer, D is the diffusion coefficient of the drug, c_{s} is the solubility of the drug, c_{ini} is the concentration of the drug initially inside the inner cavity (0.991 mol/L for nadolol and 1.15 mol/L for metoprolol), V is the total volume of the hydrogel formulation, and t is time. The solubilities in water (at 25 °C), for nadolol and metoprolol are 8330 and 402 mg/L (at 25 °C), respectively.

When the released fractions are then plotted against $\sqrt{t}$, the curves should be linear and the slopes (k) should be dependent on the area exposed to the release buffer divided by the total volume of the hydrogel. These plots are shown in Figure 4. The Eq. (1) can be further simplified to Eq. (2) by combining drug-dependent parameters variables to a constant K ($K = (Dc_{\text{s}}/c_{ini}^2(2c_{\text{ini}} - c_{\text{s}}))^{1/2}$) and drug-independent design parameters to a constant a ($a = A/V$), which is related to the geometry of the capsules.

$$f = aK\sqrt{t} = k\sqrt{t} \quad (2)$$

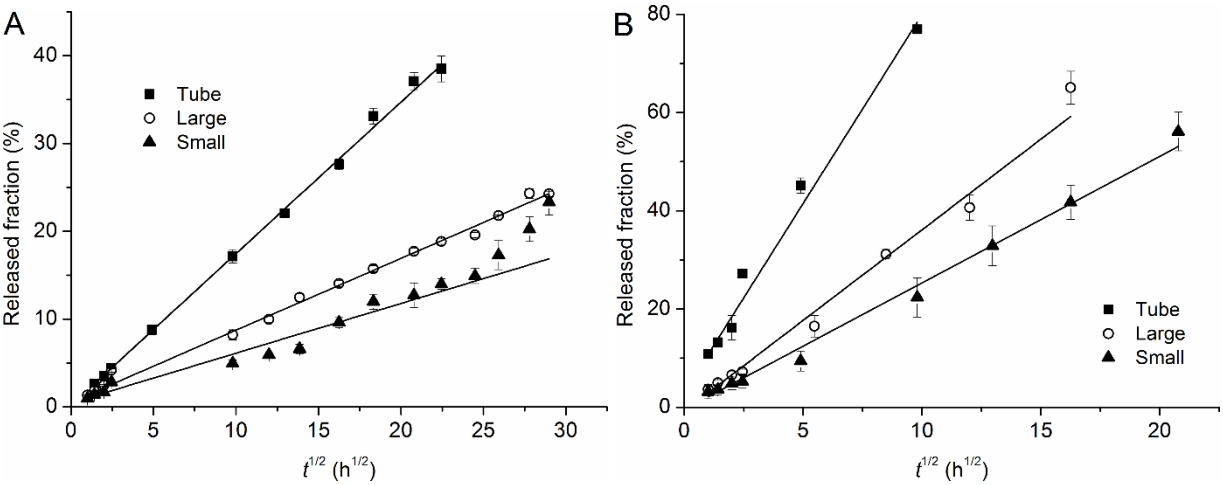

Figure 4. Fitted Higuchi equations (lines) to the nadolol (A) and metoprolol (B) release data for all three capsule designs (Tube, Large, and Small). The data points are the same as in Figure 3 but only the part of the data with no evident drug degradation was used for the fitting.

The slopes from Figure 4, and the corresponding values of the formulation parameters *a* are shown in Table 1. For metoprolol, only the parts of the release curves where no clear degradation of the drug was seen were used to do the theoretical fits. It is worth noting that in an ideal case, the release rate would be completely controlled by the design parameter *a*, as K was constant for each drug release series, however, a number of things such as swelling or more complex geometries can lead to deviations from the standard Higuchi equation. Swelling could be ruled out based on our visual observations of the capsules in buffer solutions. However, an analysis of the ratios of the slopes to the ratios of a will indicate how well the release curves fit the Higuchi equation and helps in verifying the release mechanism, since in our case we should have $a_1/a_2 = k_1/k_2$ for any two different designs.

Table 1. Slopes from the release rate fitting in Figure 4 and a comparison of the design variables (a) indicating ideal release behavior to the slopes (k) of the real release rates. The parameters are normalized to those obtained for the tube-design.

	Design parameter ratios	k		k/k_{tube}		R^2	
		Metoprolol	Nadolol	Metoprolol	Nadolol	Metoprolol	Nadolol
Tube	a/a_{tube} 1.00	7.69	1.73	1.00	1.00	0.99	1.00
Large	a/a_{tube} 0.37	3.69	0.82	0.48	0.47	0.99	1.00
Small	a/a_{tube} 0.13	2.58	0.57	0.34	0.33	0.99	0.91

All the designs could be modeled with the Higuchi equation. Especially the release data from the tube-design shows excellent near-perfect fits to Eq. (1). The equation is theoretically derived for a case very much like our current design [34]. And although the release rate from the large bottleneck is slight faster than expected, the ratio of the design parameters and the ratios of the slopes of the large and tube designs are close to each other (0.374 vs. 0.480 and 0.474), indicating similar release mechanism as in the case of the tube design. In the case of the small bottleneck, a larger deviation from theory is seen and the release rate is much faster than would have been expected (0.132 vs. 0.335). The reason is that the Higuchi equation really only describes release from the neck of the capsule, i.e. from a system with constant cross-section to volume ratio. As the bottleneck is quite short, it is not able to control the release rate alone. At some point during the release experiment, the diffusion from the larger inner cavity to the neck part will start to dominate the release kinetics. In this area, the cross section to volume ratio of the large and small designs are similar. And that is why we see that the slopes of these two designs start approaching each other later on in the release measurements. The jump to higher release fractions for the large design in the early stage

of the release is due to the difference in the cross-section to volume ratios inside the neck of the capsule.

As the release rates for several types of molecules has been measured for the same CNF hydrogel quality [16], we can estimate the release rates of various therapeutical molecules for our implant. In addition, the same CNF quality has been proven to be freeze-dryable without the loss of rheological properties nor any changes in its release profile [16]. For subcutaneous implantation the thickness of the capsules walls could be decreased for increased comfort. Despite PLA being an excellent material for the current *in vitro* tests, the material could be further enhanced to prevent foreign body reaction and bacterial growth. Recent breakthroughs include foreign body resistant materials. [35]. To prevent biofilm formation in *in vivo* environment, antimicrobial material such as nitrofurantoin can be mixed with the PLA [36-37]. In addition, the outer surface of the PLA capsule can be post-operated smoother to reduce surface area for biofilm formation [36].

4 Conclusions

In summary, the obtained leakage tests and *in vitro* results from model compounds demonstrate the suitability of the CNF hydrogel filled PLA capsules as sustained release platforms without the use of excipients. The diameter of the capsules release channel ("bottleneck") can be modified effortlessly resulting in several adjustable parameters together with the drug and hydrogel concentrations. From the theoretical analysis of the results it can be concluded that the tube and the large designs can be modeled by the Higuchi equation. As the neck is made thinner, internal diffusion kinetics become more complicated and deviations from theory are seen. Nevertheless, a

control over the release rates was maintained and the behavior of all systems can be explained by the varying cross-section to volume ratios. As the capsules are injected with the hydrogel formulations post-printing, the drug substances do not undergo heating, resulting in wide compatibility for therapeutic compounds such as proteins and liposomes. In the future, the actual injection of the hydrogel formulations could be performed automatically by 3D printers and an antimicrobial PLA feedstock could be implemented in the FDM printing.

5 Acknowledgements

The authors acknowledge and thank the University of Helsinki for co-operation and for providing access to their laboratories and screening instrumentation.

6 References

[1] Khaled, S. A., Burley, J. C., Alexander, M. R., & Roberts, C. J. (2014). Desktop 3D printing of controlled release pharmaceutical bilayer tablets. *International journal of pharmaceutics, 461*(1-2), 105-111.

[2] Sadia, M., Arafat, B., Ahmed, W., Forbes, R. T., & Alhnan, M. A. (2018). Channeled tablets: An innovative approach to accelerating drug release from 3D printed tablets. *Journal of Controlled Release, 269,* 355-363.

[3] Goyanes, A., Martinez, P. R., Buanz, A., Basit, A. W., & Gaisford, S. (2015). Effect of geometry on drug release from 3D printed tablets. *International journal of pharmaceutics*, *494*(2), 657-663.

[4] Khaled, S. A., Burley, J. C., Alexander, M. R., Yang, J., & Roberts, C. J. (2015). 3D printing of five-in-one dose combination polypill with defined immediate and sustained release profiles. *Journal of Controlled Release*, *217*, 308-314.

[5] Skorywa et al., Fabrication of extended-release patient-tailored prednisolone tablets via fused deposition modelling (FDM) 3D printing

[6]Stewart, S. A., Domínguez-Robles, J., Donnelly, R. F., & Larrañeta, E. (2018). Implantable polymeric drug delivery devices: Classification, manufacture, materials, and clinical applications. *Polymers*, *10*(12), 1379.

[7] Kleiner, L. W., Wright, J. C., & Wang, Y. (2014). Evolution of implantable and insertable drug delivery systems. *Journal of controlled release*, *181*, 1-10.

[8] Kumar, A., & Pillai, J. (2018). Implantable drug delivery systems: An overview. In Nanostructures for the Engineering of Cells, Tissues and Organs (pp. 473-511). William Andrew Publishing. KUMAR, Anoop; PILLAI, Jonathan. Implantable drug delivery

[9] Town, A. R., Taylor, J., Dawson, K., Niezabitowska, E., Elbaz, N. M., Corker, A., ... & McDonald, T. O. (2019). Tuning HIV drug release from a nanogel-based in situ forming implant by changing nanogel size. Journal of Materials Chemistry B, 7(3), 373-383.

[10] Laurén, P., Lou, Y., Raki, M., Urtti, A., Bergström, K., Yliperttula, M., 2014. Technetium-99m-labeled nanofibrillar cellulose hydrogel for in vivo drug release. Eur. J. Pharm. Sci. 65, 79–88.

[11] Kuzma, P., Moo-Young, A. J., Mora, D., Quandt, H., Bardin, C. W., & Schlegel, P. H. (1996, May). Subcutaneous hydrogel reservoir system for controlled drug delivery. In *Macromolecular Symposia* (Vol. 109, No. 1, pp. 15-26). Basel: Hüthig & Wepf Verlag.

[12] Moon, R. J., Martini, A., Nairn, J., Simonsen, J., & Youngblood, J. (2011). Cellulose nanomaterials review: structure, properties and nanocomposites. *Chemical Society Reviews*, *40*(7), 3941-3994.

[13] Plackett, D., Letchford, K., Jackson, J., & Burt, H. (2014). A review of nanocellulose as a novel vehicle for drug delivery. *Nordic Pulp & Paper Research Journal*, *29*(1), 105-118.

[14] Saito, T., Nishiyama, Y., Putaux, J. L., Vignon, M., & Isogai, A. (2006). Homogeneous suspensions of individualized microfibrils from TEMPO-catalyzed oxidation of native cellulose. *Biomacromolecules*, *7*(6), 1687-1691.

394 [15] Saito, T., Kimura, S., Nishiyama, Y., & Isogai, A. (2007). Cellulose nanofibers prepared by
395 TEMPO-mediated oxidation of native cellulose. Biomacromolecules, 8(8), 2485-2491.
396
397 [16] Paukkonen, H., Kunnari, M., Laurén, P., Hakkarainen, T., Auvinen, V. V., Oksanen, T., ... &
398 Laaksonen, T. (2017). Nanofibrillar cellulose hydrogels and reconstructed hydrogels as matrices
399 for controlled drug release. International journal of pharmaceutics, 532(1), 269-280.
400
401 [17] Gupta, P., Vermani, K., & Garg, S. (2002). Hydrogels: from controlled release to pH-
402 responsive drug delivery. Drug discovery today, 7(10), 569-579.
403
404 [18] Kolakovic, R., Peltonen, L., Laukkanen, A., Hirvonen, J., & Laaksonen, T. (2012).
405 Nanofibrillar cellulose films for controlled drug delivery. European Journal of Pharmaceutics and
406 Biopharmaceutics, 82(2), 308-315.
407
408 [19] Alhnan, M. A., Okwuosa, T. C., Sadia, M., Wan, K. W., Ahmed, W., & Arafat, B. (2016).
409 Emergence of 3D printed dosage forms: opportunities and challenges. *Pharmaceutical research*,
410 *33*(8), 1817-1832.
411
412 [20] Pham, D. T., & Gault, R. S. (1998). A comparison of rapid prototyping technologies.
413 *International Journal of machine tools and manufacture*, *38*(10-11), 1257-1287.
414
415 [21] Gaylo, C. M., Pryor, T. J., Fairweather, J. A., & Weitzel, D. E. (2006). *U.S. Patent No.*
416 *7,027,887*. Washington, DC: U.S. Patent and Trademark Office.

[22] Genina et. al. Anti-tuberculosis drug combination for controlled oral delivery using 3D printed compartmental dosage forms: From drug product design to in vivo testing. J Control Release. 2017 Dec 28; 268:40-48. doi: 10.1016/j.jconrel.2017.10.003.

[23] Itzoe, M., & Guarnieri, M. (2017). New developments in managing opioid addiction: impact of a subdermal buprenorphine implant. Drug design, development and therapy, 11, 1429.

[24] Ling, W., Casadonte, P., Bigelow, G., Kampman, K. M., Patkar, A., Bailey, G. L., ... & Beebe, K. L. (2010). Buprenorphine implants for treatment of opioid dependence: a randomized controlled trial. *Jama*, *304*(14), 1576-1583.

[25] Slaughter, B. V., Khurshid, S. S., Fisher, O. Z., Khademhosseini, A., & Peppas, N. A. (2009). Hydrogels in regenerative medicine. Advanced materials, 21(32-33), 3307-3329.

[26] McFarland, J. W., Avdeef, A., Berger, C. M., & Raevsky, O. A. (2001). Estimating the water solubilities of crystalline compounds from their chemicall structures alone. Journal of chemical information and computer sciences, 41(5), 1355-1359.

[27] Chinga-Carrasco, G., & Syverud, K. (2014). Pretreatment-dependent surface chemistry of wood nanocellulose for pH-sensitive hydrogels. *Journal of biomaterials applications*, *29*(3), 423-432.

[28] Lin, N., & Dufresne, A. (2014). Nanocellulose in biomedicine: Current status and future prospect. *European Polymer Journal*, *59*, 302-325.

[29] Powell, L. C., Khan, S., Chinga-Carrasco, G., Wright, C. J., Hill, K. E., & Thomas, D. W. (2016). An investigation of Pseudomonas aeruginosa biofilm growth on novel nanocellulose fibre dressings. *Carbohydrate polymers*, *137*, 191-197.

[30] Zhang, Y., Nypelö, T., Salas, C., Arboleda, J., Hoeger, I. C., & Rojas, O. J. (2013). Cellulose nanofibrils. *1*, *3*, *1*(3), 195-211.

[31] Boetker, J., Water, J. J., Aho, J., Arnfast, L., Bohr, A., & Rantanen, J. (2016). Modifying release characteristics from 3D printed drug-eluting products. *European Journal of Pharmaceutical Sciences*, *90*, 47-52.

[32] Wang, L., Xu, H., Cooper, W. J., & Song, W. (2012). Photochemical fate of beta-blockers in NOM enriched waters. *Science of the total environment*, *426*, 289-295.

[33] Siepmann, J., & Siepmann, F. (2012). Modeling of diffusion controlled drug delivery. *Journal of Controlled Release*, *161*(2), 351-362.

[34] Siepmann, J., & Peppas, N. A. (2011). Higuchi equation: derivation, applications, use and misuse. *International journal of pharmaceutics*, *418*(1), 6-12.

[35] Farah, S., Doloff, J. C., Müller, P., Sadraei, A., Han, H. J., Olafson, K., ... & Griffin, M. (2019). Long-term implant fibrosis prevention in rodents and non-human primates using crystallized drug formulations. Nature Materials, 1.

[36] Sandler, N., Salmela, I., Fallarero, A., Rosling, A., Khajeheian, M., Kolakovic, R., ... & Vuorela, P. (2014). Towards fabrication of 3D printed medical devices to prevent biofilm formation. International journal of pharmaceutics, 459(1-2), 62-64.

[37] Water, J. J., Bohr, A., Boetker, J., Aho, J., Sandler, N., Nielsen, H. M., & Rantanen, J. (2015). Three-dimensional printing of drug-eluting implants: preparation of an antimicrobial polylactide feedstock material. *Journal of pharmaceutical sciences*, *104*(3), 1099-1107.